

Creation of the second neutrino laboratory at the SM-3 reactor in order to increase the accuracy of the „Neutrino-4“ experiment

© A.P. Serebrov,¹ V.G. Ivochkin,¹ R.M. Samoïlov,¹ A.K. Fomin,¹ V.G. Zinoviev,¹ S.S. Volkov,¹ V.L. Golovtsov,¹ N.V. Gruzinskii,¹ P.V. Neustroev,¹ V.V. Fedorov,¹ I.V. Parshin,¹ A.A. Gerasimov,¹ M.E. Zaytsev,^{1,3} M.E. Chaikovskii,¹ A.M. Gagarskiy,¹ A.L. Petelin,² A.L. Izhutov,² M.O. Gromov,² S.A. Sazontov,² A.A. Tuzov,² V.I. Ryikalin,⁴ D.A. Makarenkov,⁵ A.M. Nemeryuk,⁵ T.E. Kuzmina⁶

¹ Petersburg Nuclear Physics Institute, National Research Center „Kurchatov Institute“, Gatchina, Russia

² JSC „State Science Center Research Institute of Atomic Reactors“, Dimitrovgrad, Russia

³ Dimitrovgrad Engineering and Technological Institute MEPhI, Dimitrovgrad, Russia

⁴ A.A. Logunov Institute for High Energy Physics of the National Research Center „Kurchatov Institute“, 142281 Protvino, Moscow Region, Russia

⁵ NRC „Kurchatov Institute“ — IHEP, Protvino, Russia

⁶ JSC Radium Institute. V.G. Khlopina, St. Petersburg, Russia

e-mail: serebrov_ap@npfi.nrcki.ru

Received November 2, 2022

Revised November 2, 2022

Accepted November 2, 2022

In the experiment „Neutrino-4“ on the search for a sterile neutrino, the effect of oscillations was found at a confidence level of 3 standard deviations. In order to significantly increase the accuracy of the experiment, a second neutrino laboratory is created at the SM-3 reactor (Dimitrovgrad, Russia) and a new neutrino detector is developed. The scintillation-type detector consists of 4 modules having a multi-sectional structure with a horizontal arrangement of 100 sections with PMTs located on both sides of the section. The possibility of increasing the accuracy of the experiment by a factor of 2.7 is shown, which will make it possible to achieve a confidence level of more than 5 standard deviations and answer the question of the existence of a sterile neutrino.

Keywords: sterile neutrino, reactor antineutrino.

DOI: 10.21883/TP.2023.01.55452.241-22

Introduction

It is assumed, that owing to a reactor antineutrino transition to a sterile state, the oscillation effect at a short reactor distance and deficiency of a reactor antineutrino flux at a long range are likely to be observed. The above-described properties of the new particle make it one of candidates for the dark matter and require to extend the framework of our understanding of the elementary particle interaction and look beyond the limits of the Standard Model. Thus, the research activities related to neutrino, especially to the reactor antineutrino, give an accessible possibility to search for the new physics. Anomalies are found in a number of accelerator and reactor experiments: LSND [1], MiniBooNE [2], reactor anomaly [3], as well as in GALLEX/GNO, SAGE, and BEST experiments with radioactive sources [4–6]. Finally, in the „Neutrino-4“ experiment an oscillation effect was observed with parameters of $\Delta m_{14}^2 = 7.3 \text{ eV}^2$ and $\sin^2 2\theta = 0.36$ at the confidence level of 2.9σ [7]. Therefore, a considerable increase in experiment accuracy is needed. For this purpose the second neutrino laboratory and a detector with a 2.7 times higher sensitivity are being created at the SM-3 reactor. This will allow achievement of a confidence level greater than 5 standard deviations and answer the question of sterile neutrino existence.

1. The „Neutrino-4“ experiment

The main goal of „Neutrino-4“ experiment is to search for the oscillation of reactor antineutrino to a sterile state. The experiment sensitivity to possible parameter values is strongly dependent on the source size. Thus, for example, for the reactor core size of a power plant commercial reactor the sensitivity to region with a mass squared difference greater than 6 eV^2 is considerably decreased. Therefore, of great importance are the experiments on research reactors with a small core, which can be considered as a point source for the measurement of neutrino flux at the distances in question.

Due to its compact core ($42 \times 42 \times 35 \text{ cm}$) and highly enriched fuel, the SM-3 research reactor is one of the best places to carry out the experiment to search for oscillations at short distances. It has an advantage in comparison with commercial reactors with their too large cores and heterogeneous composition of fuel, which is differently burnable. In addition, laboratory rooms are separated from each other by thick concrete walls.

The „Neutrino-4“ experiment is carried out since the end of 2013 at SM-3 reactor of JSC SSC RIAR, in the neutrino laboratory, room 162 (Fig. 1), that was created at the same time. The idea of this experiment consists in the use of a mobile sectioned detector to measure antineutrino

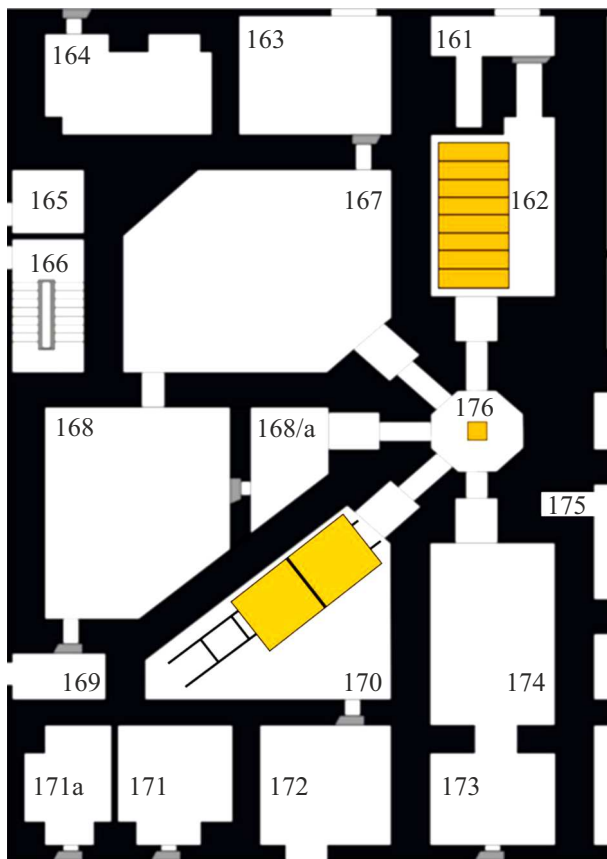


Figure 1. Horizontal plan of the SM-3 reactor building. Orange rectangle at the top (in the on-line version) — detector in neutrino laboratory No. 1, orange rectangle at the bottom (in the on-line version) — detector under development in neutrino laboratory No. 2.

flux and spectra at different distances from the reactor. This direct observation of spectra allows for a model-independent analysis and therefore has an advantage in comparison with the experiments that require engagement of calculated spectra or a precise evaluation of the number of antineutrino produced in the reactor core. During the time of „Neutrino-4“ experiment, we have obtained for the first time in the world the oscillation effect at a confidence level of about three standard deviations in the region of $\Delta m_{14}^2 = 7.3 \text{ eV}^2$ and $\sin^2 2\theta = 0.36$. To confirm this result, an experiment accuracy improvement is needed.

2. Neutrino laboratory No. 2

The major difficulty to achieve this goal is the fact that the reactor is located on the Earth's surface and the laboratory rooms are exposed to a strong impact of the space radiation that creates a background of fast neutrons. In respect to the task of antineutrino detection, it is a high level of correlated background from fast neutrons. Sectioning of the detector allowed for a twice higher ratio of effect/background and achievement of a level of 0.5,

but it is still not enough. Notwithstanding that the statistics acquisition with the existing detector will be continued to proceed with the understanding of the nature of the reactor anomaly and the phenomenon of neutrino oscillations into a sterile state, a development of the „Neutrino-4“ experiment is needed, which is related first of all with suppression of the correlated background and the accidental coincidence background. Therefore, a decision was made to create a new setup with improved sensitivity and place it in another room of the SM-3 reactor. In room 170 at the SM-3 reactor there is a possibility to measure the antineutrino flux even in a wide range of distances (6–15 m), than in the existing laboratory. Base length of the experiment plays an important role in the model-independent analysis when searching for oscillations, because it allows normalizing to a spectrum averaged over the total base, without significant distortion to the oscillation dependence.

In this respect, the issue arises as to creation of the second neutrino laboratory in room 170 and the use of additional methods of controlling both the correlated background through the pulse shape discrimination of signals, improvement of the active shielding efficiency, optimization of the passive shielding, and the suppression of the accidental coincidence background through the increased concentration of gadolinium. On this basis we can formulate requirements for the new system to detect reactor antineutrino, which is planned to be implemented in room 170 (Fig. 1).

First, the measurements should be carried out by four identical detectors on a mobile platform. This will allow us to cover all the range of distances and improve statistical accuracy of the experiment.

Second, the following technologies should be implemented in the new detectors:

- sectioned structure of detectors, which already proved to be effective in the measurements with a model and a full-scale detector;
- each section should be observed by PMT from both sides, which will allow for the use of the technique of pulse shape discrimination of signal and improve energy resolution of the detector;
- application of the technique of pulse shape discrimination (the use of appropriate scintillator, PMT, and electronics);
- the use of scintillator with a greater concentration of gadolinium to suppress the accidental coincidence background;
- the use of internal active shielding in a geometry close to the 4π -geometry.

Meeting the above-listed requirements for detectors is necessary to implement the plans for neutrino flux and neutrino spectrum measurements in a range of 6–15 m from the reactor in order to establish causes of the reactor anomaly and to determine allowed values of the parameter of oscillations into a sterile state.

Currently, room 170 at the SM-3 reactor is prepared for the detector accommodation.

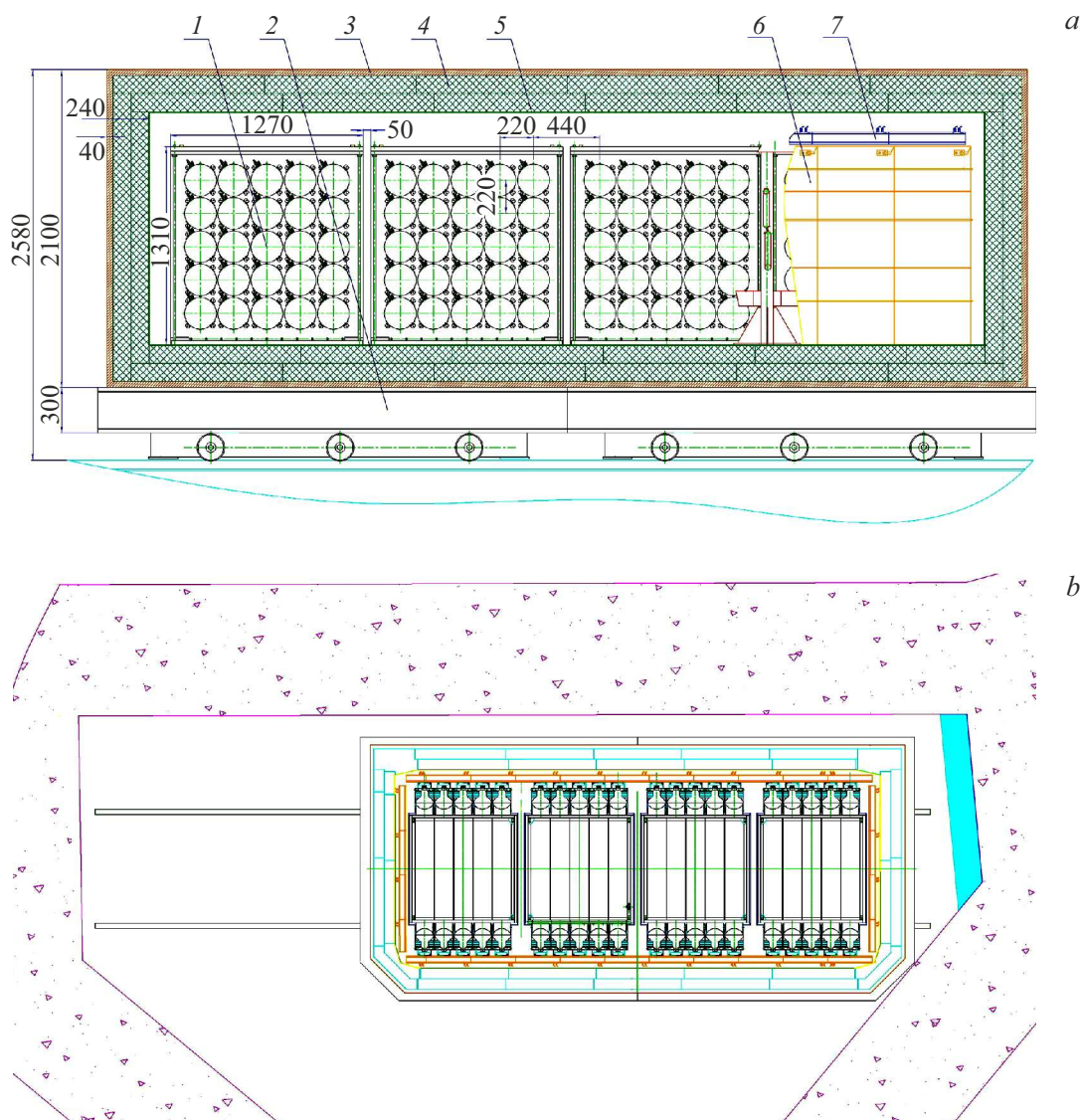


Figure 2. *a* — design of the reactor antineutrino detector on a mobile platform; *b* — diagram of detectors arrangement in room 170: 1 — antineutrino detector, 2 — mobile platform, 3 — copper, 4 — borated polyethylene, 5 — borated rubber, 6 — vertical panels of the active shielding, 7 — top panels of the active shielding.

3. Design of the new detector

The detector is composed of four identical modules located on a mobile platform together with the active and passive shielding (Fig. 2). Due to the detector's movement, all the range of distances to the reactor core will be covered. Each of four modules is composed of 5×5 horizontal sections of $21.6 \times 21.6 \times 116.6$ cm with securely fixed partitions between them. The partitions serve to prevent the light from output beyond the section limits. When carrying out measurements, the detector will move to different positions over distances, which will be multiples of the section size. The gap between modules is equal to the section size. Thus, each point will be measured by different sections and possible difference in the efficiency of detector sections will be averaged. The sections are filled

with liquid scintillator. The scintillator material is mineral oil with an addition of gadolinium. Each section has 2 PMTs located on its ends. The liquid scintillator is separated from the PMT by a transparent plexiglas wall with a thickness of 3 cm. There is a cylinder lightguide between the wall and the PMT. There is no optical contact, there is an air gap between the PMT surface and the transparent wall.

The scintillation-type detector is based on the use of the inverse beta decay reaction: $\bar{\nu}_e + p \rightarrow e^+ + n$. A positron emitted in an inverse beta decay process annihilates with the emission of two gamma quanta, each having an energy of 511 keV and opposite directions. A resulted neutron is absorbed by the gadolinium with emission of a cascade of gamma quanta with a sum energy of about 8 MeV. The detector will register two successive signals from the positron and neutron — so called correlated events serving

as the signal that an antineutrino is recorded. In the first-order approximation the relation between positron and antineutrino energy is linear: $E_{\bar{\nu}} = E_{e^+} + 1.8 \text{ MeV}$. Therefore, the antineutrino spectrum in the experiment is derived from the positron spectrum.

Thus, the antineutrino flux from the reactor is measured as a function of distance and energy in order to search for the neutrino oscillations, that are manifested in the spectrum change at different distances.

4. Study of the passive shielding of the antineutrino detector

There are two background sources: the gamma background of natural radioactivity and the background of space radiation. The gamma-background of natural radioactivity creates a problem related to the accidental coincidence, because an antineutrino is registered by a signal from positron and a signal from neutron capture in a certain time interval. The space background creates the problem of correlated coincidence events from fast neutrons created as a result of the interaction between space muons and substance nuclei.

So, fast neutrons are the cause of the correlated background, and gamma-radiation and thermal neutrons are the source of the accidental coincidence background. Protection against these types of radiation uses polyethylene, borated polyethylene, borated rubber — shielding against thermal and fast neutrons, while lead, iron, and copper protect against the gamma-radiation. The main difficulty is that lead, iron, and copper, being heavy elements with large nucleon number, have a high suppression factor of gamma-radiation, however, they are themselves sources of fast neutrons, which are created in the process of interaction between nuclei of these elements and hard muon component of the space radiation. This disadvantage is related to lead to the most significant extent.

To investigate optimum composition of the passive shielding, we used a model of antineutrino detector passive shielding. Detectors of gamma-radiation and neutron radiation or a mockup of antineutrino detector section with liquid scintillator were placed inside the mockup.

4.1. Studying the suppression of gamma-background

30-mm lead shielding outside the polyethylene shielding with a thickness of 80 mm suppresses the gamma-background inside approximately by an order of magnitude in virtually the same manner throughout the entire spectrum. By adding another 80 mm of polyethylene and 10 mm of Pb inside the shielding, a gamma-background suppression factor of approximately 20 times can be achieved, and in this case placing lead inside results in a better suppression of the soft (below 500 keV) part of the spectrum (Fig. 3).

4.2. Studying the suppression of neutron background

A proportional ^3He -counter was used as a detector of thermal neutrons. Results of measurements with this detector for different options of shieldings are presented in Table 1.

Table 1 presents results for six configurations of shielding against neutrons.

In configuration 1 (open detector) the count rate of thermal neutrons was $0.68 \pm 0.008 \text{ s}^{-1}$. This count rate is assumed as a unit for the calculation of the suppression factor of neutron count rate or the shielding efficiency.

In configuration 2 (detector wrapped in two layers of borated rubber with a thickness of 5 mm) the count rate of thermal neutrons was $0.009 \pm 0.0004 \text{ s}^{-1}$, while the suppression factor was 75 times. It should be noted, that this suppression factor is referred to thermal neutrons only. The shielding against fast neutrons requires polyethylene to thermalize fast neutrons with their subsequent capture by boron.

In configuration 3 (detector in a shielding of pure polyethylene) even a 1.2 times increase in the thermal neutron count rate is observed due to the thermalization of fast neutrons.

Protection configuration 4 (detector in a shielding of borated polyethylene (5%)) is, of course, the most effective, and the suppression factor in this case is 26.8 times.

It is rather evident that the use of borated rubber inside will yield a significant increase in the suppression factor. Indeed, in configuration 5 (two layers of borated rubber inside the shielding of borated polyethylene) the count rate was $0.0027 \pm 0.00013 \text{ s}^{-1}$, and the suppression factor of thermal neutrons was 251 times. It is this configuration that should be considered optimum.

Finally, configuration 6 demonstrates that placing a lead shielding outside the shielding results in an increase in neutron count rate by 10 times in relation to configuration 4 without lead. The cause is that space mesons produce a considerable number of fast neutrons on heavy lead nuclei, which are extremely harmful because these neutrons can yield correlated events.

Nevertheless, the external gamma-shielding is necessary and iron or copper can be used as a compromise. We decided to use copper, because the configuration of magnetic field inside an iron shielding can be nonhomogeneous and change over time. This is necessary in order to avoid the magnetic field influence on PMT.

We have simulated the muon interaction for two shielding options: made of copper (Cu) and lead (Pb). Both metals effectively suppress the external background of gamma-radiation, therefore we compared their influence on the production of secondary neutrons as a result of the interaction with muons.

The major portion of the muon background at the Earth's surface is within a range of 0.1–3 GeV. We considered normal incidence of muon flux with different energies on

Table 1. Suppression of neutron background for six configurations of shielding

Sketch	Description of shielding	Neutrons, s^{-1} Suppression factor
1 	Open detector	0.68 ± 0.008 1.0
2 	Detector wrapped in two layers of borated rubber	0.009 ± 0.0004 75
3 	Detector in a shielding made of pure polyethylene. Sheet thickness is 60 mm	0.8086 ± 0.003 0.84
4 	Detector in a shielding made of borated polyethylene. Sheet thickness is 80 mm	0.0254 ± 0.0006 26.8
5 	Two layers of borated rubber are placed in the shielding made of borated polyethylene	0.0027 ± 0.00013 251
6 	Shielding made of borated polyethylene is coated with three layers of lead (30 mm) from outside	0.2418 ± 0.001 2.8

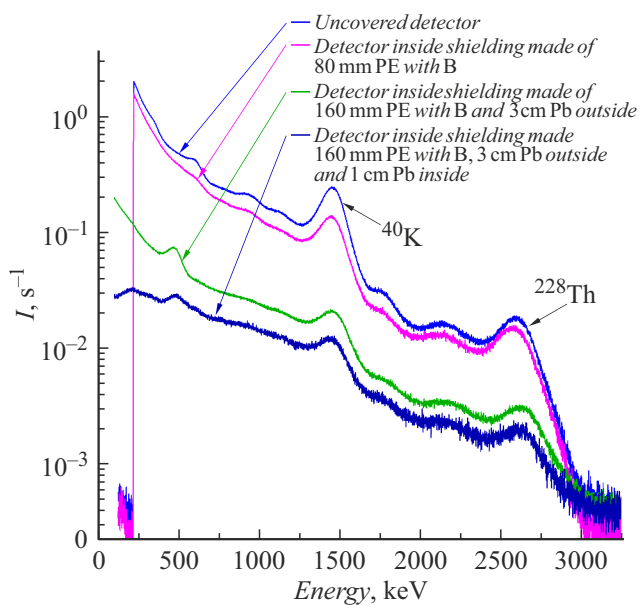


Figure 3. Spectra of the gamma-radiation background in a room on the Earth's surface, registered by a BDEG2-39 detector placed inside different options of shielding. The first two curves demonstrate, that polyethylene, which is extremely important for the shielding against neutrons, has nearly no contribution to the shielding against gamma-radiation. The second two curves demonstrate the effect of gamma-background suppression by lead outside and inside the polyethylene shielding. Peaks of the spectrum are related to the natural radioactivity of ^{40}K and ^{228}Th , as well as 511 keV from the annihilation of positrons.

a metal layer with a thickness of 50 mm. The simulation was carried out in GEANT4 software. Muons can be split into two categories: muons with energies over 0.2 GeV, that pass through the metal layer and interact with nuclei when passing, and muons with energies below 0.15 GeV, that are

highly likely to be stopped in the metal and captured by metal nuclei. These two cases differ from each other by type of the interaction that produces neutrons, and should be considered independently.

For the case of muon energies over 0.2 GeV the total number of neutrons produced by muon passage in a range of 0.2–5 GeV through lead is 3 times higher than that through copper. For muons with energies below 0.3 MeV the production of neutrons has a very low probability in comparison with that for higher energies: the number of neutrons for both metals increases with growth of the muon energy. On average over the considered range of energies lead also produces 3 times larger numbers of neutrons, than copper.

5. Measurement of the accidental coincidence background and the background of correlated events using the mockup of detector section at different options of passive and active shielding

In addition to the shielding made of lead, borated polyethylene, and borated rubber, an active shielding (AS) is used to suppress the background, which consists in plates of plastic scintillator where optic fibers are laid, a light-sensitive cell with necessary electronics is mounted.

The use of AS both inside and outside reduces the accidental coincidence background by 1.6 times without external and internal passive shielding (PS). Thus, we select the option of internal AS, because it is the most compact. With an external PS (6 cm of lead and 3 cm of steel) the accidental coincidence background with switched on internal AS is suppressed by 3 times, at the same time the accidental coincidence background is decreased by 3.3 times due to the

external PS (before the AS is switched on). As a result, the accidental coincidence background is decreased by 10 times due to the external PS and internal AS.

As for the counting rate of correlated coincidence events, its suppression is more difficult to achieve. The correlated coincidence background is increased with the use of PS, especially the internal PS. However, this increase can be compensated by the AS switching on.

6. Pulse shape discrimination of signal

The correlated coincidence background arises due to fast neutrons, that, when scattered on hydrogen, produce recoil protons and then, after thermalization, are captured by gadolinium nuclei, that emit gamma quanta. This process simulates the process of antineutrino registration, where first a registration of positron and gamma quanta takes place, and then, with a certain delay, a neutron is registered after the capture by gadolinium, which emits gamma quanta. The registration of a positron and gamma quanta results in a fast signal, and the registration of a recoil proton results in a signal with an additional slow tail.

The pulse shape discrimination (PSD) of signals is carried out by plotting the distribution of $\frac{Q_{tail}}{Q_{total}}$ for the sum pulse from all PMTs, where Q_{tail} — signal integral starting from some place to the end of pulse, Q_{total} — total integral of the signal. To characterize the pulse shape discrimination we used FOM (Figure of merit) parameter,

$$FOM = \frac{\mu_2 - \mu_1}{fwhm_1 + fwhm_2},$$

where μ_i — expected value, the position of appropriate Gaussian peak, and $fwhm_i$ — its half width, $fwhm_i = 2\sqrt{2 \ln 2} \sigma \approx 2.35\sigma$. The starting place of pulse tail integration is selected such that the largest FOM is achieved. With $FOM \leq 0.3$ peaks are superimposed each other and nearly can not be discriminated, with $FOM \geq 1$ peak discrimination is clear enough.

Properties of the following scintillators were compared: Chinese scintillator (sample 1), Korean scintillator NEOS (sample 2), Chinese scintillator with addition of 9% diisopropylnaphthalene (DIN) (sample 3), IREA scintillator (sample 4), IREA scintillator Naphthalene 0.5%Gd (sample 5), and IREA scintillator Benzothiofene 0.5%Gd (sample 6).

Scintillator properties were investigated in a setup with two PMTs located in the close vicinity to the vessel with scintillator, above which a Pu–Be-neutron source is placed that radiates not only neutrons, but also gamma quanta (Fig. 4). Neutrons and gamma quanta can be discriminated by pulse shape. The scintillator, which is planned for use, was developed in the IREA.

Fig. 4 shows distributions of the $\frac{Q_{tail}}{Q_{total}}$ parameter for IREA scintillator (sample 4) and for the Korean scintillator NEOS (sample 2). To compare light yields of each sample, we measured energy spectrum of the ^{22}Na gamma-radiation

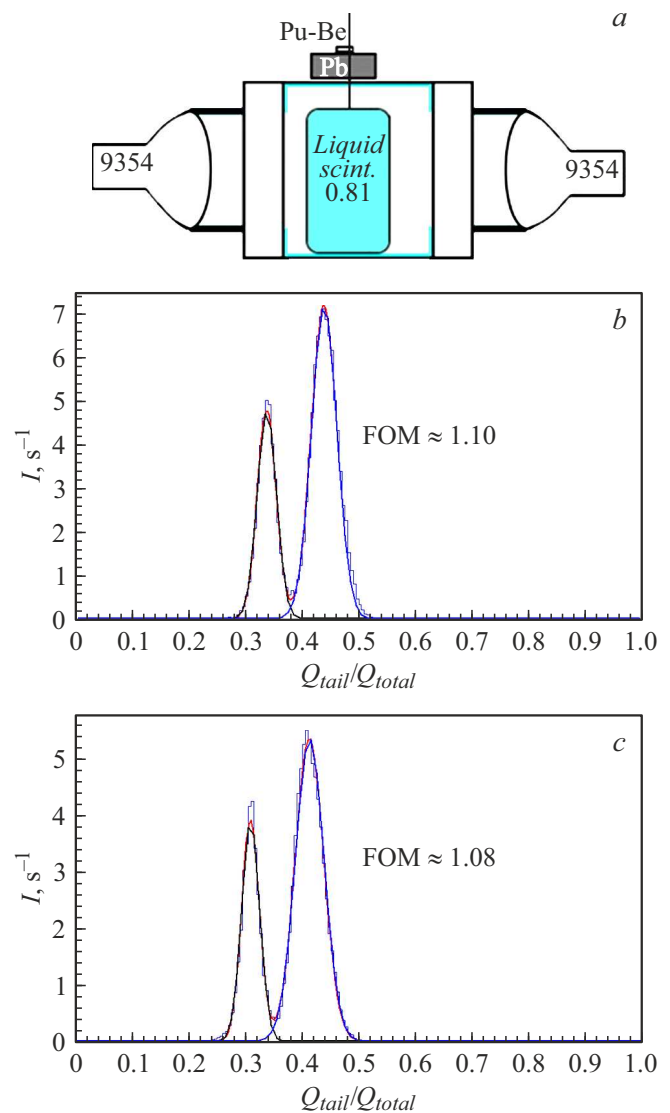


Figure 4. *a* — diagram of setup for studying properties of scintillators with two PMTs located in close vicinity to the vessel with scintillator; *b* — distribution of $\frac{Q_{tail}}{Q_{total}}$ for the IREA scintillator with addition of DIN (9%); *c* — the same for the NEOS scintillator.

source. Positions of the middle of the last falling part of spectra were compared. In addition, thermal neutron capture time was measured for each sample. Data for all samples is presented in Table 2.

Gadolinium concentration in the IREA scintillator is 2 g/l. This will allow reduction of the time interval between correlated signals, which will result in a reduction of the accidental coincidence background by ~ 1.8 –2 times. Further increase in gadolinium concentration, although it will give even stronger decrease in the accidental coincidence background, but can result in scintillator instability, turbidity or settling of sediment, therefore we are limited by a Gd concentration of 0.2%.

Table 2. Comparative characteristics of scintillator samples

Samples	Chinese Daya Bay 0.1% Gd	Korean 0.5% Gd	Chinese Daya Bay DIN 9% 0.1% Gd	IREA DIN 9% 0.2% Gd	IREA Naphthalene 0.5% Gd	IREA Benzothiophene 0.5% Gd
	1	2	3	4	5	6
FOM	0.66	1.08	0.94	1.10	0.87	1.06
1274 keV, channels	310	280	260	280	310	145
$\tau, \mu\text{s}$	43.8	16.4	40.0	21.1	14.7	12.8

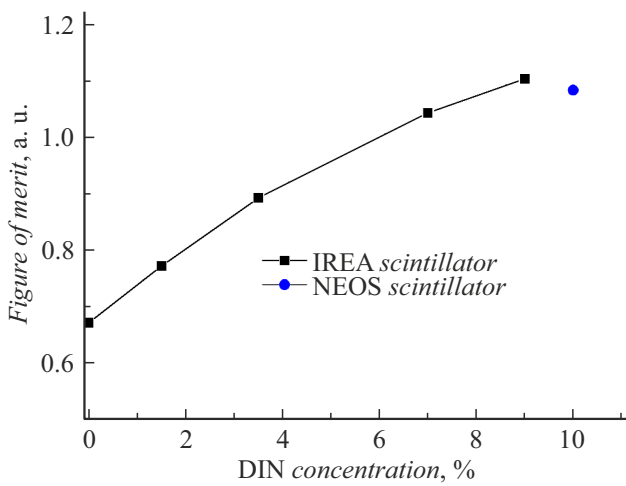


Figure 5. Dependence of the pulse shape discrimination by FOM on DIN concentration for NEOS and IREA scintillators.

Also, we have investigated the dependence of FOM on the concentration of DIN for the IREA scintillator based on linear alkylbenzene (LAB), which is shown in Fig. 5.

The pulse shape discrimination of signals depends not only on the scintillator, but also on the detector design in general. The system used to select the scintillator composition has the optimum design to achieve maximum possible pulse discrimination. For a real detector section the discrimination will be worse due to the leading edge smoothing caused by the lightguide elongation. Fig. 6 shows scheme of PSD parameters measurement, that allows evaluating the actual discrimination of signals for a real section. This scheme corresponds to one section of the detector. The transparent container with liquid scintillator was installed inside the lightguide of the section with PMTs (Fig. 6).

By comparing the results obtained from the measurements on the section for the IREA scintillator with addition of 9% DIN and for the NEOS scintillator (Fig. 6), a conclusion can be made that the IREA scintillator is a fully-featured replacement for the NEOS scintillator, from which a required level of suppression of the correlated background from fast neutrons can be expected through the pulse shape discrimination technique.

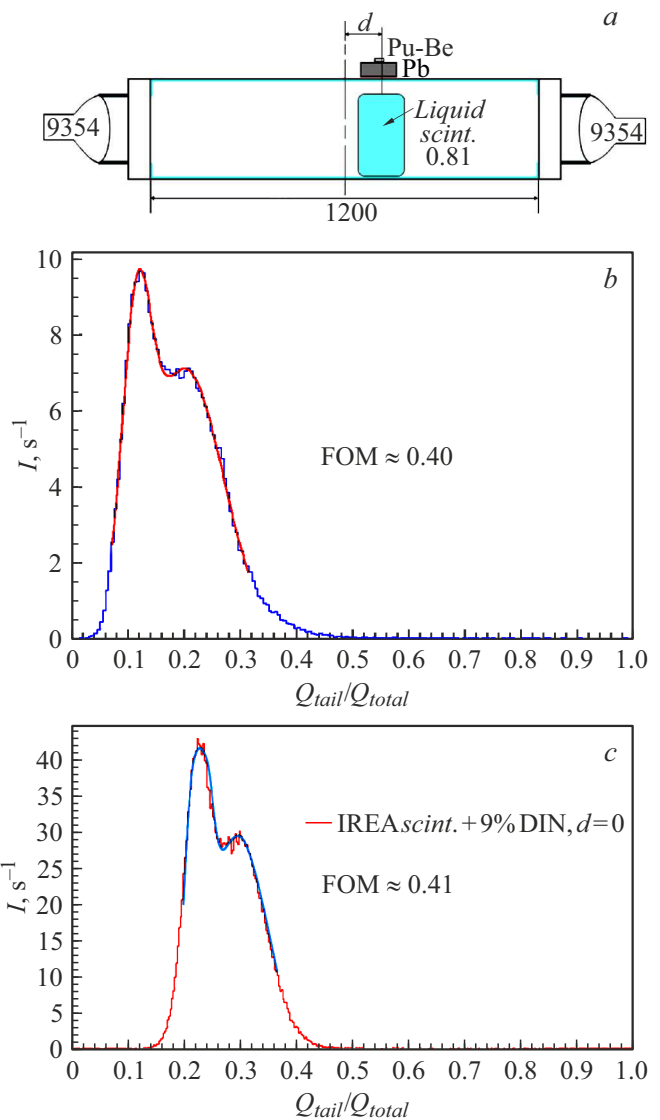


Figure 6. a — diagram to measure PSD parameter for the scintillator inside the detector section; b — for the NEOS scintillator inside the section; c — distribution of $\frac{Q_{tail}}{Q_{total}}$ for the IREA scintillator with 9% of DIN.

7. Investigation of the scheme with two photomultipliers

The idea to use the configuration with two PMTs pursues the following two goals: to improve the light collection

quality due to the symmetrical geometry and to reduce the noise level due to the use of coincidence scheme.

In these investigations we have used the model of one section, which diagram is shown in Fig. 6. The lightguide was filled with scintillator, and a GAGG-scintillator (gadolinium–aluminum–gallie garnet doped with cerium provided by JSC „Fomos-Materialy“, Moscow) was used as a source of light, with ^{241}Am inside that was a source of α -particles with an energy of 5.5 MeV. The signal from this light source has an amplitude distribution with a half width of 8%, and the pulse shape features a slow component, that allows discriminating these signals by the pulse shape.

This source was moved along the lightguide axis. The dependence of signal amplitude distribution was measured for each PMT and for their sum on the light source position.

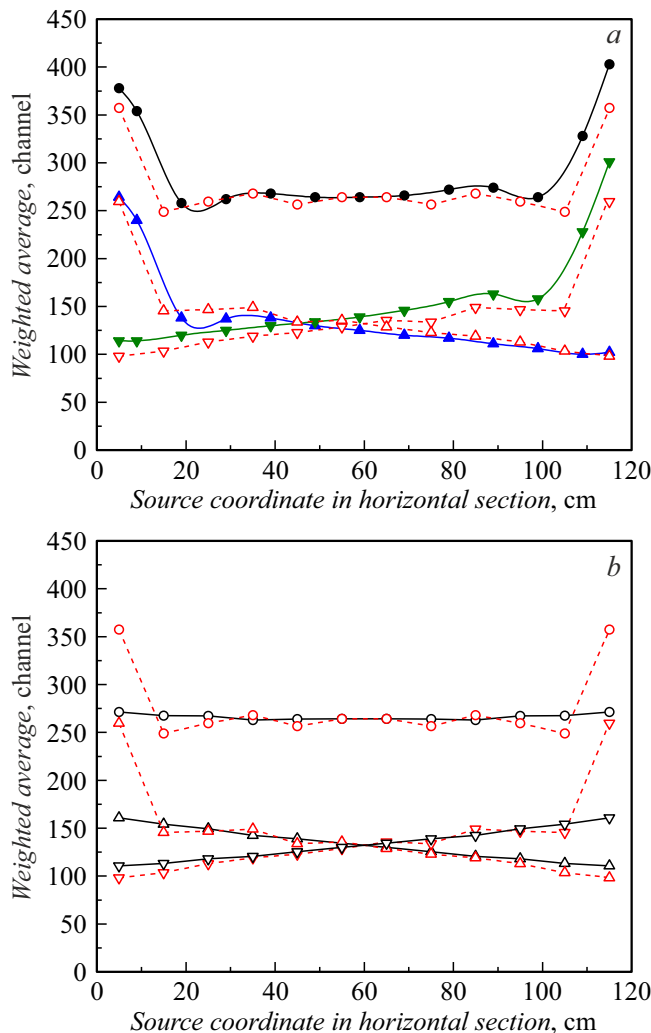


Figure 7. *a* — dependence of weighted average value of light source signals on the distance along the lightguide axis for the sum signal of coincidences and for each PMT individually, but subject to the existence of coincidences (filled triangles — experiment, empty triangles — calculation); *b* — the same dependence calculation for the lightguide cross-section (results of calculation for the cross-section are connected by solid line, results for the axis are connected by dashed line).

The same dependencies were calculated for the light source along the lightguide axis and for the lightguide cross-section.

It can be seen, that due to the symmetry of the scheme a compensation of light collection efficiency takes place for different points of the detector. Exceptions are the extreme points located on the lightguide axis. However, calculations for the cross-section show that the effect disappears. The matter is that the rectangular lightguide has its ends closed with mirrored walls with holes, which diameters are equal to the PMT diameter. Therefore, the light out of this orifice plate does not enter the PMT. This compensates for the excess of light in the zone nearest to PMT (Fig. 7).

Thus, for the configuration with two PMTs, the light collection is homogeneous enough over the cross-section of the light guide. This is a good result. However, as it will be shown below, the energy distribution for the neutrino events recording is mainly defined by the incomplete recording of the 511 keV gamma quanta within the section.

8. Simulating the experiment

8.1. Energy resolution of the detector

To simulate the experiment, a Monte Carlo model was developed, where trajectory is calculated for each of the photons that are generated from the inverse beta decay reaction with the recording of positron, i.e. with absorption of antineutrino by proton. We used the reactor antineutrino spectrum for uranium-235 in our calculations. The direction of positron escape is assumed to be isotropic. The exponential length of photon path in the scintillator is 4 m for the calculation. Photons are reflected from walls in specularly with a reflection probability of 0.95.

Fig. 8, *a* shows in the form of color diagram the amplitude of PMT signal as a function the place of positron event with a positron energy of 4 MeV. The efficiency of light transportation for right angles of incidence on the mirror walls of the lightguide is worse due to multiple reflection between walls, therefore the light from far positions reaches the PMT less well than the light from near positions. However, in the configuration with two PMTs on opposite sides activated for coincidence this effect is compensated. Exceptions are the regions near PMTs.

Fig. 8, *b* shows the distribution of PMT count rate (number or recorded photons) from positrons of different energies at incompletely recorded energy release from 2 gamma quanta of 511 keV each. Width of the distribution is almost independent on the positron energy and equal 500 keV. This is defined mainly by the incomplete absorption of gamma quanta within the section. The distribution splitting into two peaks at low energies is explained by this circumstance as well. Using the data from Fig. 8, it is possible to establish the connection between photons and the positron energy.

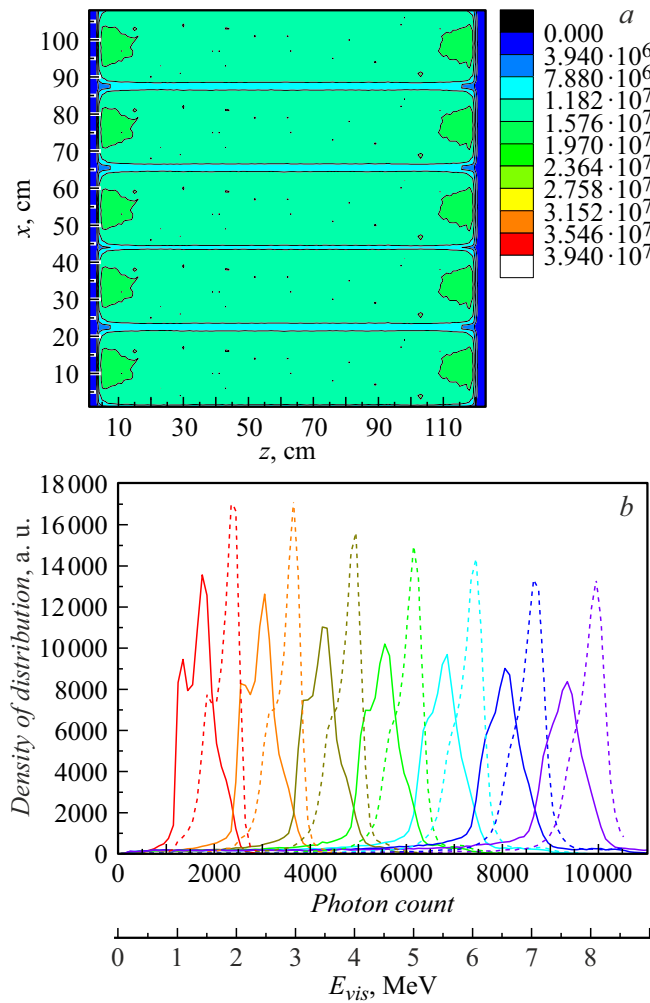


Figure 8. *a* — color diagram, count rate of PMTs of detector sections depending on the place of positron event with a positron energy of 4 MeV; *b* — distribution of PMT count rate from positrons with an energy from 1 to 7 MeV taking into account the incomplete recording of 511 keV gamma quanta — solid line. Taking into account signals from 511 keV gamma quanta in neighboring sections allows improvement of the energy resolution of antineutrino recording — dashed line (recording threshold in neighboring sections is 100 keV).

8.2. Simulation of antineutrino flux, event matrix, and oscillation curve

The experiment uses a method based on relative measurements that exclude the shape of spectrum, i.e. model-independent data analysis. The method is based on the use of the following equation:

$$R_{ik}^{\text{exp}} = (N_{ik} \pm \Delta N_{ik}) L_k^2 / K^{-1} \sum_k (N_{ik} \pm \Delta N_{ik}) L_k^2,$$

where R_{ik} — element of the event matrix, numerator in the right part is the count of antineutrino events with a set energy corrected for the factor of L^2 , denominator is the count of antineutrino events with the same set energy

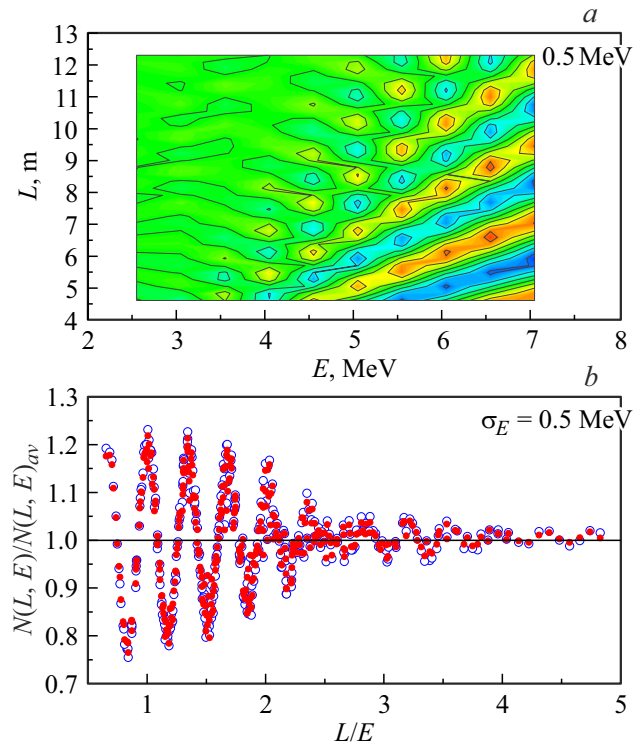


Figure 9. *a* — event matrix — probability of antineutrino recording depending on the energy and distance; *b* — oscillation curve, red dots (in the on-line version) correspond to the real geometry with finite dimensions of the reactor core ($42 \times 42 \times 35$ cm) and detector sections ($21.6 \times 21.6 \times 116.6$ cm), blue circles (in the on-line version) correspond to the almost ideal case, i.e. with dimensions less by an order of magnitude; σ_E — energy resolutions.

averaged over all distances, i — number of the energy interval, k — number of the distance interval.

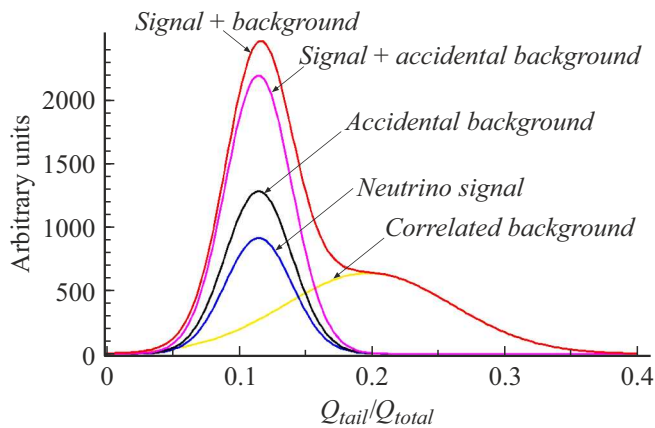
The antineutrino flux was simulated taking into account sizes of the reactor core and its spatial position in relation to the antineutrino detector. Antineutrinos are produced uniformly in the volume of the reactor core with an isotropic escape direction. It was assumed that the antineutrino beam is directed parallel to the detector axis. This assumption is possible, provided that the detector is 6–15 m away from the reactor core. The simulation is carried out over the entire distance with a 0.23 m step of detector motion and an antineutrino energy resolution of 0.5 MeV.

As a result of the simulation an even matrix was obtained. Fig. 9, *a* shows in the form of color diagram the distribution of probability of antineutrino events recording as a function of energy and distance.

The data sampling is to be carried out over the L/E parameter, because it is the parameter on which the effect of oscillations depends on. This is the method of so called coherent summation of measurement results, that opens the possibility of direct observation of antineutrino oscillations thanks to the data sampling over variable L/E . By summing

Table 3. Factors that improve measurement accuracy in the new laboratory in comparison with the existing laboratory

Method	Consequences of application	Coefficient
4 detectors	3 times higher volume	1.6
Concentration of Gd is 0.2%	2 times lower accidental coincidence	1.3
Pulse shape	4 times lower correlated coincidence	1.3
Total		2.7

**Figure 10.** Expected distribution of the PSD-parameter for correlated signals in the new neutrino detector in the SM-3 reactor.

events with the same values of L/E , an oscillation curve can be obtained, which is shown in Fig. 9, *b*.

Number of oscillations on the curve is defined by the energy resolution. The simulation of the oscillation curve used an energy resolution of 500 keV, which, as it was shown above, is almost independent on the positron energy and defined mainly by the absorption of gamma quanta within the section. With this energy resolution the number of observed oscillations is 4–5.

The effect of oscillations attenuation is mainly defined by the energy resolution of the detector. The influence of finite dimensions of the core and dimensions of sections on the oscillations attenuation effect is considerably less in relation to the influence of the energy resolution of the detector (Fig. 9, *b*).

9. Calculation of accuracy of the experiment on oscillations detection

In new detectors it is planned to engage methods to suppress the correlated background and the space radiation background that haven't been used before. The section structure implemented in the existing detector allowed improvement of the effect/background ratio from 0.3 to 0.6 and partial suppression of the accidental coincidence background (by 2.5 times). The use of the configuration with two PMTs on each side of the section along with the use

of scintillator with good properties of pulse shape discrimination will give an opportunity to apply this technique to discriminate neutrino events from background events related to fast neutrons.

In addition, gadolinium concentration in this scintillator is 2 times higher than that in the scintillator, which is currently in use. The comparison between the scintillator with a gadolinium concentration of 0.1% and a similar scintillator with a concentration of 0.2% has shown that due to the proportional reduction of the time window for the delayed signal search the accidental coincidence background in the same conditions is decreased almost by 2 times.

As the measurements with the mockup of new detector section show, the use of signal discrimination from heavy and light particles will allow up to 2 times improvement of the effect/background ratio. That is, the suppression of the correlated background will be even 4 times. A three-times increase in the scintillator volume respectively will allow speeding up the statistic data collection.

The influence of above-listed factors that improve measurement accuracy in the new laboratory in comparison with the existing one and the final estimate of the accuracy improvement are presented in Table 3.

Conclusion

In this work we have presented the results of preparatory experiments for the creation of a new detector for the second neutrino laboratory on the SM-3 reactor.

The study of passive shielding of the antineutrino detector against gamma radiation has shown that although the use of lead is very effective, especially in the low-energy part of the spectrum, however it is not acceptable because fast neutrons produced from the interaction between space radiation muons and lead nuclei are a source of the correlated background. Nevertheless, the external gamma-shielding is necessary and iron or copper can be used as a compromise.

The study of neutron shielding has shown that the use of borated polyethylene (5%) only is insufficient, and borated rubber (40%) is additionally required in the cavity to absorb the thermal neutrons produced after thermalization of the fast neutrons of polyethylene.

The use of AS inside the passive shielding is preferable, because it is more compact and reduces the level of signal load on detectors. With an external PS (6 cm of lead

and 3 cm of steel) the accidental coincidence background with switched on internal AS is suppressed by 3 times, and in combination with the direct PS effect the accidental coincidence background is decreased by 10 times.

As for the counting rate of correlated coincidence events, its suppression is more difficult to achieve. The correlated coincidence background is increased with the use of PS, especially the internal PS. However, this increase can be compensated by the AS switching on.

The correlated coincidence background is extremely harmful, therefore another method must be applied, i.e. the pulse shape discrimination of signals. The LAB-based scintillator with addition of DIN manufactured by IREA is as good as the NEOS scintillator that was planned for the use earlier.

The configuration of detector sections with two PMTs on each side of the section along with the use of scintillator with good properties of pulse shape discrimination will give an opportunity to apply the technique of discrimination of neutrino events from background events related to fast neutrons.

All these advantages make it possible to improve the experiment accuracy by 2.7 times, which will allow achievement of a confidence level greater than 5σ . Thanks to the creation of neutrino laboratory No. 2 on the SM-3 reactor and a new detector, the final answer will be given for the question on the existence of a sterile neutrino with the parameters of oscillations observed in the „Neutrino-4“ experiment.

Funding

The study was funded by a grant from the Russian Science Foundation (project № 20-12-00079) and with support by a grant of the Ministry of Science and Higher Education of the Russian Federation (Agreement № 075-11-2021-073 of 16.09.2021).

Conflict of interest

The authors declare that they have no conflict of interest.

References

- [1] A. Aguilar, L.B. Auerbach, R.L. Burman, D.O. Caldwell, E.D. Church, A.K. Cochran, J.B. Donahue, A. Fazely, G.T. Garvey, R.M. Gunasingha, R. Imlay, W.C. Louis, R. Majkic, A. Malik, W. Metcalf, G.B. Mills, V. Sandberg, D. Smith, I. Stancu, M. Sung, R. Tayloe, G.J. VanDalen, W. Vernon, N. Wadia, D.H. White, S. Yellin. *Phys. Rev. D*, **64**, 112007 (2001). DOI: 10.1103/PhysRevD.64.112007
- [2] A.A. Aguilar-Arevalo, B.C. Brown, L. Bugel, G. Cheng, J.M. Conrad, R.L. Cooper, R. Dharmapalan, A. Diaz, Z. Djurcic, D.A. Finley, R. Ford, F.G. Garcia, G.T. Garvey, J. Grange, E.-C. Huang, W. Huelsnitz, C. Ignarra, R.A. Johnson, G. Karagiorgi, T. Katori, T. Kobilarcik, W.C. Louis, C. Mariani, W. Marsh, G.B. Mills, J. Mirabal, J. Monroe, C.D. Moore, J. Mousseau, P. Nienaber, J. Nowak, B. Osmanov, Z. Pavlovic, D. Perevalov, H. Ray, B.P. Roe, A.D. Russell, M.H. Shaevitz, J. Spitz, I. Stancu, R. Tayloe, R.T. Thornton, M. Tzanov, R.G. Van de Water, D.H. White, D.A. Wickremasinghe, E.D. Zimmerman. *Phys. Rev. Lett.*, **121**, 221801 (2018). DOI: 10.1103/PhysRevLett.121.221801
- [3] G. Mention, M. Fechner, Th. Lasserre, Th.A. Mueller, D. Lhuillier, M. Cribier, A. Letourneau. *Phys. Rev. D*, **83**, 073006 (2011). DOI: 10.1103/PhysRevD.83.073006
- [4] W. Hampel, G. Heusser, J. Kiko, T. Kirsten, M. Laubenstein, E. Pernicka, W. Rau, U. Rönn, C. Schlosser, M. Wójcik, R.V. Ammon, K.H. Ebert, T. Fritsch, D. Heidt, E. Henrich, L. Stieglitz, F. Weirich, M. Balata, F.X. Hartmann, M. Sann, E. Bellotti, C. Cattadori, O. Cremonesi, N. Ferrari, E. Fiorini, L. Zanotti, M. Altmann, F.V. Feilitzsch, R. Mößbauer, G. Berthomieu, E. Schatzman, I. Carmi, I. Dostrovsky, C. Bacci, P. Belli, R. Bernabei, S. d'Angelo, L. Paoluzi, A. Bevilacqua, M. Cribier, L. Gosset, J. Rich, M. Spiro, C. Tao, D. Vignaud, J. Boger, R.L. Hahn, J.K. Rowley, R.W. Stoerner, J. Weneser. *Phys. Lett. B*, **420**, 114 (1998). DOI: 10.1016/S0370-2693(97)01562-1
- [5] J.N. Abdurashitov, V.N. Gavrin, S.V. Girin, V.V. Gorbachev, T.V. Ibragimova, A.V. Kalikhov, N.G. Khairnasov, T.V. Knodel, V.N. Kornoukhov, I.N. Mirmov, A.A. Shikhin, E.P. Veretenkin, V.M. Vermul, V.E. Yants, G.T. Zatsepin, Yu.S. Khomyakov, A.V. Zvonarev, T.J. Bowles, J.S. Nico, W.A. Teasdale, D.L. Wark, M.L. Cherry, V.N. Karaulov, V.L. Levitin, V.I. Maev, P.I. Nazarenko, V.S. Shkol'nik, N.V. Skorikov, B.T. Cleveland, T. Daily, R. Davis, Jr., K. Lande, C.K. Lee, P.S. Wildenhain, S.R. Elliott, J.F. Wilkerson. *Phys. Rev. C*, **59**, 2246 (1999). DOI: 10.1103/PhysRevC.59.2246
- [6] V.V. Barinov, S.N. Danshin, V.N. Gavrin, V.V. Gorbachev, D.S. Gorbunov, T.V. Ibragimova, Yu.P. Kozlova, L.V. Kravchuk, V.V. Kuzminov, B.K. Lubsandorzhiyev, Yu.M. Malyshekin, I.N. Mirmov, A.A. Shikhin, E.P. Veretenkin, B.T. Cleveland, H. Ejiri, S.R. Elliott, I. Kim, R. Massarczyk, D. Frekers, W.C. Haxton, V.A. Matveev, G.V. Trubnikov, J.S. Nico, A.L. Petelin, V.A. Tarasov, A.I. Zvir, R.G.H. Robertson, D. Sinclair, J.F. Wilkerson. *Phys. Rev. C*, **105**, 065502 (2022). DOI: 10.1103/PhysRevC.105.065502
- [7] A.P. Serebrov, R.M. Samoïlov, V.G. Ivochkin, A.K. Fomin, V.G. Zinoviev, P.V. Neustroev, V.L. Golovtsov, S.S. Volkov, A.V. Chernyj, O.M. Zherebtsov, M.E. Chaikovskii, A.L. Petelin, A.L. Izhutov, A.A. Tuzov, S.A. Sazontov, M.O. Gromov, V.V. Afanasiev, M.E. Zaytsev, A.A. Gerasimov, V.V. Fedorov. *Phys. Rev. D*, **104**, 032003 (2021). DOI: 10.1103/PhysRevD.104.032003